Proceedings of the 28th IEEE
EMBS Annual International Conference
New York City, USA, Aug 30-Sept 3, 2006

Neural Interface Dynamics Following Insertion of Hydrous Iridium Oxide Microelectrode Arrays

Matthew D. Johnson, *Student Member, IEEE*, Nicholas B. Langhals, *Student Member, IEEE*, and Daryl R. Kipke, *Member, IEEE*

***Abstract*—Studies examining traumatic brain injury have suggested a 'window of opportunity' exists for therapeutic agents to mitigate edema and cellular toxicity effectively. However, successful therapy also relies on identifying the extent of blood-brain barrier disruption, which is associated with excessive extra-cellular concentrations of ions, excitatory amino acids, and serum proteins. The following study investigates the use of pH-selective hydrous iridium oxide microelectrodes to assess trauma following insertion of a neural probe. Electrochemical activation of iridium microelectrode arrays was performed in either acidic (0.5 M H_2SO_4) or weak basic (0.3 M Na_2HPO_4, pH = 8.56) solutions. Both oxides demonstrated super-Nernstian pH sensitivity (-88.5 mV/pH and -77.1 mV/pH, respectively) with little interference by other cations. Data suggest that acid-grown oxide provides better potential stability than base-grown oxide (σ = 2.8 versus 4.9 mV over 5 hours). Implantation of these electrodes into motor cortex and dorsal striatum revealed significant acidosis during and following insertion. Variability in the spatiotemporal pH profile included micro-scale inhomogeneities along the probe shank and significant differences in the averaged pH response between successive insertions using the same depth and speed. This diagnostic technology has important implications for intervention therapies in order to more effectively treat acute surgical brain trauma.**

I. Introduction

Implantable microelectrode arrays provide unique interfaces to record neural activity for treatment of certain neurological disorders and diseases [1, 2]. As this technology translates to clinical applications, ensuring the long-term functionality of these devices is a critical consideration. Numerous studies have demonstrated an inherent variability in spike recording quality during the first few weeks of implant, after which only a fraction of electrode sites remain functionally active [3-7]. We hypothesize that insertion trauma accounts for part of this variability.

The act of inserting a probe into brain tissue inevitably disrupts microvasculature, resulting in increased permeability of endothelial cells and their tight junctions to serum proteins, glutamate, ions, and other species [8, 9].

Manuscript received April 24, 2006. This work was supported by the NIH NIBIB under grant EB005022-01A1 and by the NSF Engineering Resource Center for Wireless Integrated Microsystems (WIMS) under grant EEC-9986866.

M. D. Johnson, N. B. Langhals, and D. R. Kipke are with the Department of Biomedical Engineering, University of Michigan, Ann Arbor, MI 48109 USA (phone: 734-647-2123; fax: 734-936-1905; e-mail: mdjzz@umich.edu, langhals@umich.edu, and dkipke@umich.edu).

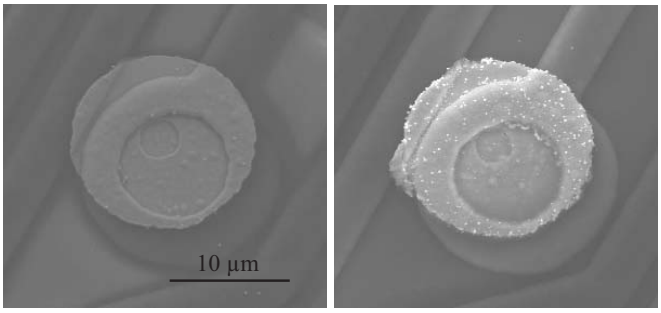

Fig. 1. SEM images of 177 µm^2 microelectrode sites consisting of iridium (left) and hydrous iridium oxide (right).

The ensuing ionic gradient imbalance is often associated with vasogenic edema, or an increase in extracellular water content that leads to abnormally high intracranial pressures [10]. As documented in traumatic brain injury (TBI) patients and animal models, intervention strategies to limit the extent of edema and neurotoxicity have a limited window of opportunity from 1-12 hours [11]. Consequently, determining the extent of blood-brain barrier (BBB) disruption may provide a beneficial feedback mechanism for managing acute surgical brain trauma.

To monitor cellular trauma, we have developed a novel microelectrode array with recording sites selective to pH and capable of recording extra-cellular electrophysiological activity from nearby neurons. The electrode material consisted of hydrous iridium oxide, previously shown to be sensitive to pH via an oxycation equilibrium reaction [12-14]. The results demonstrate a significant variability in neural interface dynamics among probe insertions.

II. Materials and Methods

A. Surgical Procedures

Nine male Sprague-Dawley rats (250-300 g) were anesthetized with an intraperitoneal cocktail of ketamine (50 mg/mL), xylazine (5.0 mg/mL) and acepromazine (1.0 mg/mL) and maintained with ketamine updates. Rats were positioned in a stereotaxic frame, whereby a craniotomy was made over motor cortex. Stainless steel bone screws (316SS) were placed posterior to these craniotomies. Probes were then implanted into cortex or dorsal striatum [15]. All procedures complied with the NIH guidelines for the care and use of laboratory animals and with the University of Michigan Committee on Use and Care of Animals.

B. Probe Fabrication and Packaging

Silicon-substrate microelectrode arrays with thin-film iridium contact sites were fabricated through the Center for Neural Communication Technology at the University of Michigan (Fig. 1). The arrays consisted of a single 1 cm-long shank with sixteen 700 μm^2 sites separated by 100 µm. Arrays were attached to a 16-channel printed circuit board (PCB) with hot wax. Array bond pads were then wire-bonded with gold wire to the PCB and insulated with a silicone elastomer (MED-4211; Nusil Technology, Carpenteria, CA).

C. Electrochemical Techniques

Hydrous iridium oxide films were formed electrochemically in either 0.5 M H_2SO_4 or in 0.3 M Na_2HPO_4 (pH of 8.56) with an Autolab PGSTAT12 potentiostat (Eco Chemie; Utrecht, Netherlands). Acid-grown iridium oxide ($IrOx_A$) formation involved applying a 0.5 Hz square wave between +1.25 V and -0.25 V to each microelectrode site for 800 cycles. The final cycle stopped at +1.25 V for better interface stability [12]. Base-grown iridium oxide ($IrOx_B$) formation consisted of a 1 Hz square wave between +0.90 V and -0.85 V for 200 cycles. These potentials were in reference to a saturated calomel electrode (SCE).

The thin films were characterized by cyclic voltammetry (CV) before and after oxide formation in both the activation solution and in 0.1 M phosphate buffered saline (PBS) adjusted to pH 7.4. Voltammograms ranged from +1.00 to 0.00 V for acid-grown oxide and from +0.75 to -0.25 V for base-grown oxide. Arrays were rinsed in DI water, allowed to dry for 15 minutes, and then dipped three times for 2 seconds in Nafion, a perfluorinated cation-exchange resin (Sigma-Aldrich; St. Louis, MO). After a 24-hour dry time in a dark container, the arrays were soaked for an additional 24 hours in 0.1 M PBS to re-hydrate and homogenize the oxycations at the microelectrode surface [16].

Potentiometric recordings were low-pass filtered at 3 Hz and acquired through either the Autolab potentiostat, a 4-channel BioStat (ESA Biosciences; Chelmsford, MA), or a custom 16-channel electrometer. Microelectrode sites were calibrated for pH (6 to 9) using aliquots of HCl and NaOH in 0.1 M PBS. The solution pH was monitored concurrently with a Corning combination pH and temperature electrode and a Corning pH meter 440 (Corning Electrochemical Products; Woburn, MA). Selectivity analysis involved characterizing the arrays with infusions of NaCl (50 µM to 50 mM), KCl (50 µM to 50 mM), $CaCl_2$ (40 µM to 15 mM), and $MgCl_2$ (50 µM to 30 mM) into 0.1 M PBS. *In vivo* potentiometric recordings were in reference to an Ag/AgCl electrode positioned in a cortical cup filled with 0.1 M PBS over the craniotomy.

D. Electrophysiological Recordings

Extracellular recordings consisted of voltage-time series data sets sampled at 25 kHz with 16-bit resolution on a multichannel acquisition system (TDT, Alachua, FL). Recordings were in reference to a 316SS bone screw implanted posterior to lambda and made on the same microelectrode sites as in the potentiometric measurements. During recording sessions, rats were placed in an electrically shielded chamber. Electrophysiological data were analyzed offline using Plexon Off-line Sorter (Plexon, Dallas, TX), NeuroExplorer (Nex Techologies, Littleton, MA), and MATLAB (Mathworks, Natick, MA).

III. Results

The following set of experiments examined interface stability of Ir, $IrOx_A$, and $IrOx_B$ microelectrode sites. We then applied these sensors to examine extra-cellular pH dynamics and electrophysiological activity during vasogenic edema in rat brain.

A. Improved Interface Stability

Electrochemical characteristics of the three electrode surface types revealed significant differences in terms of potential stability. Prior to and after oxide formation, arrays were placed in 0.1 M PBS for five hours to monitor drift in the open circuit potential (Table I). Again, measurements were in reference to an SCE. $IrOx_A$ showed a significantly lower variance (2.844 ± 0.004 mV) than Ir (21.161 ± 0.176 mV, one-way ANOVA, p = 0.0003) and marginally lower variance compared to $IrOx_B$ (4.867 ± 0.006, one-way ANOVA, p = 0.0428). Cyclic voltammograms of both iridium surface treatments demonstrated differences in the redox potentials of the Ir^{3+}/Ir^{4+} transition, indicating

TABLE I
STABILITY OF IRIDIUM SURFACE TREATMENTS

Surface	n	OCP mean (mV)	OCP variance (mV)
Ir	23	359.2 ± 72.0	21.2 ± 13.2
$IrOx_A$	9	139.3 ± 4.1	2.8 ± 1.9
$IrOx_B$	14	125.9 ± 7.3	4.9 ± 2.4

OCP: open circuit potential

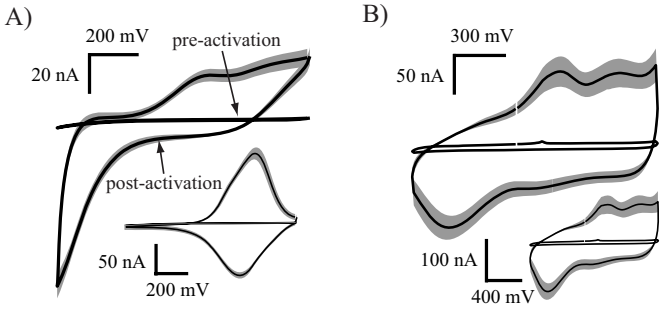

Fig. 2. Electrochemical characteristics of iridium oxide activated in 0.5 M H_2SO_4 and 0.3 M Na_2HPO_4. (A) $IrOx_A$ cyclic voltammagrams in 0.1 M PBS and 0.5 M H_2SO_4 (inset) showed significant increases in charge carrying capacity after activation. The latter voltammagram shows clear Ir^{3+}/Ir^{4+} transition with similar oxidation and reduction potentials. Gray fills represent the standard deviation of n = 15 sites. (B) Cyclic voltammagrams of $IrOx_B$ in 0.1 M PBS and 0.3 M Na_2HPO_4 (inset). Oxidation and reduction peaks were offset. Again, gray fills represent standard deviation of n = 15 sites.

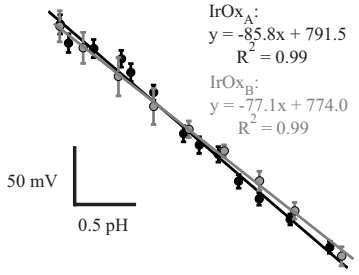

Fig. 3. Both $IrOx_A$ and $IrOx_B$ demonstrated super-Nernstian pH sensitivity (above) and selectivity over other cation species (right).

TABLE II
SELECTIVITY OF IRIDIUM SURFACE TREATMENTS

Cation	$IrOx_A$			$IrOx_B$		
	n	Sensitivity (mV/decade)	p-value	n	Sensitivity (mV/decade)	p-value
H^+	15	-85.8 ± 2.9	<0.001	4	-77.1 ± 1.6	<0.001
Na^+	10	-1.5 ± 1.2	0.004	14	-1.5 ± 0.1	<0.001
K^+	10	-0.1 ± 0.5	0.251	15	-0.5 ± 0.1	<0.001
Ca^{2+}	10	0.8 ± 0.8	0.005	13	1.77 ± 0.9	0.101
Mg^{2+}	10	-2.6 ± 0.5	0.144	15	-3.6 ± 1.0	0.010

different oxide configurations (Fig. 2). Both oxides were sensitive to pH in the super-Nernstian range (Fig. 3, -85.8 and -77.1 mV/decade for $IrOx_A$ and $IrOx_B$, respectively), unresponsive to other cations released during vasogenic edema (Table II), and responsive to quick pH fluctuations (~0.03 pH units/s).

B. pH Dynamics following Probe Implantation

Based on the *in vitro* results, a series of hydrous iridium oxide ($IrOx_A$) microelectrode arrays were implanted with a computer-controlled piezoelectric actuator system into motor cortex (2 mm deep) or dorsal striatum (6 mm deep) at user-defined insertion speeds (50 µm/s to 1 mm/s). Substantial acidosis was evident following insertion with immediate pH troughs ranging from 6.14 to 7.33 and ten minute post-implant pH responses varying between 6.31 to 7.57 (n=356). An example 2 mm deep, 50 µm/s insertion is shown in Fig. 4A with its corresponding spatiotemporal response plot shown in Fig. 4B. In this case, a gradient response was evident with more significant acidosis farther up the probe shank. While this phenomenon was evident in a number of insertions, other pH dynamics were also observed including more significant acidosis midway along the shank (Fig. 4C). Implant variability in acidosis-associated blood-brain barrier disruption was also evident by comparing pH response profiles averaged across 16 sites (Fig. 4D).

C. Relating pH Dynamics with Neural Activity

To investigate how these pH dynamics relate to neural activity, arrays implanted acutely in rat motor cortex recorded pH and high-speed electrophysiological activity concurrently across four sites. pH waveforms exhibited typical acidosis troughs and recoveries following probe insertion (Fig. 5A). Multi-unit activity displayed high amplitude action potentials initially, which subsided into lower amplitude burst firing within 500 s (Fig 5B). These first-order experiments demonstrate the ability to apply these microsensors to investigate how pharmacological changes in extracellular pH affect neural activity and similarly how neural firing activity affects the local pH microenvironment.

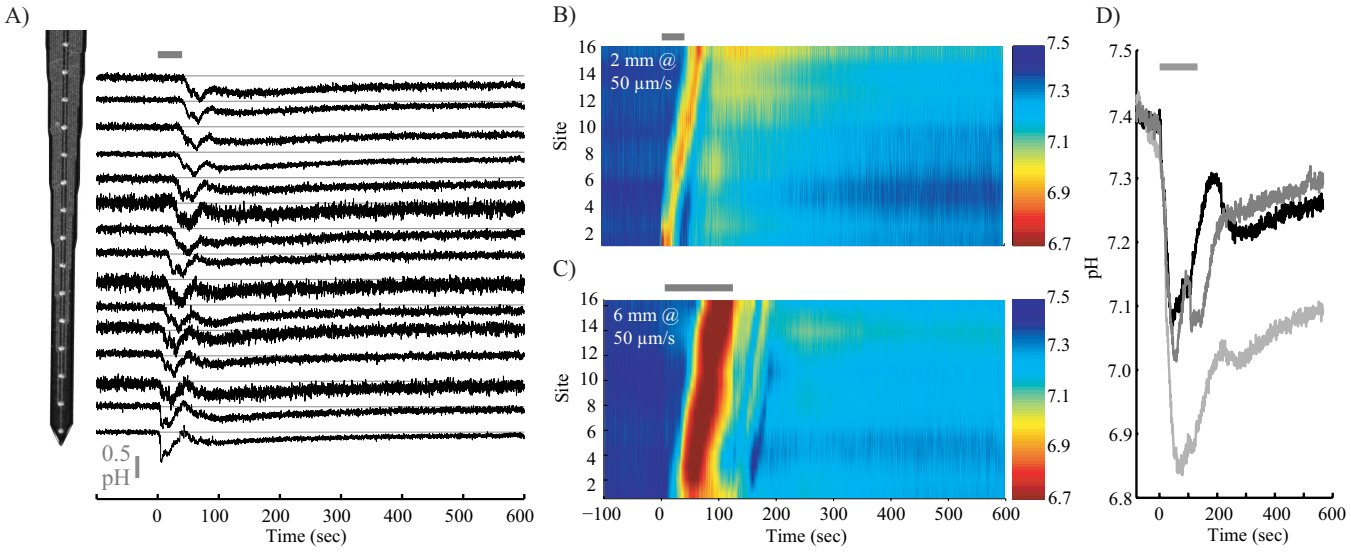

Fig. 4. pH dynamics following insertion of a neural microelectrode array. (A) In this example, 15 sampled channels recorded significant decreases in pH following insertion with a slow return to a pH of ~7.3. (B) The corresponding spatiotemporal plot further showed that proximal sites recorded more prolonged acidosis. Though, as in (C), other insertions demonstrated more significant acidosis at sites midway along the shank. (D) Variability was evident among insertions using the same implantation technique, shown for three consecutive 6 mm-deep, 50 µm/s implants. Gray bars indicate time of insertion.

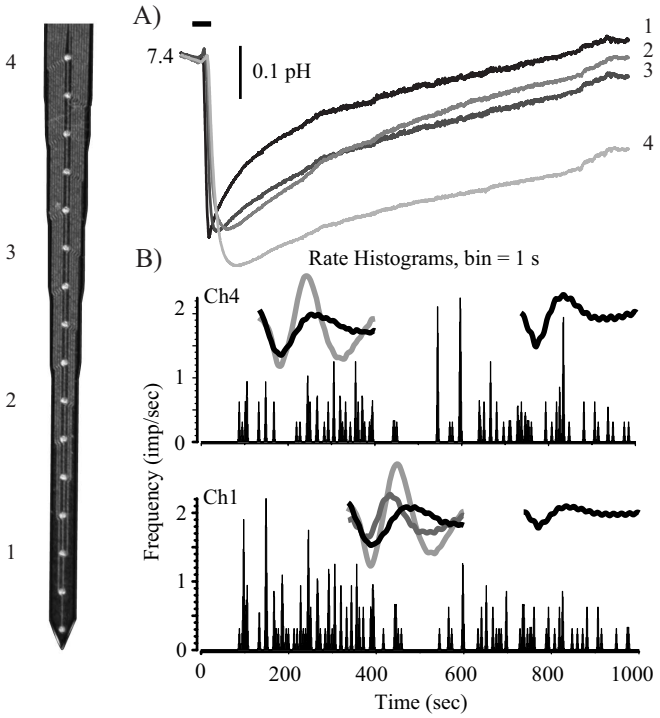

Fig. 5. Concurrent potentiometric pH and unit activity recordings following probe implantation denoted by the solid black bar. (A) For this implant, a more prolonged acidosis response was evident on proximal sites. (B) Unit activity, as shown for sites 1 and 4, was predominantly aperiodic burst firing.

IV. Discussion

Given that acute damage to neural tissue during probe insertion may lead to chronic symptoms of poor device performance – cellular edema and neuronal apoptosis – assessing and minimizing trauma during the surgical procedures is highly significant. This paper describes a novel tool to measure pH and electrophysiological activity simultaneously with hydrous iridium oxide electrodes. This is particularly relevant as acidosis associated with brain trauma has a correlation with negative clinical outcome [17].

Iridium oxide can exist in an anhydrous or hydrous state, depending on the method of deposition. Thermal and sputtered deposition creates compact anhydrous layers, which consist of a mixture of IrO_2 and Ir_2O_3. These layers, however, are often prone to open circuit potential drifting. Burke and Scannell showed the oxide structure depended on the activation solution, with base-grown oxide exhibiting a more amorphous conformation [12, 13]. Acid-grown oxide consisted of crystalline-like layers with a much greater capacity for material dispersion due to H_2O recrystallization layers. It is also not surprising that these forms of iridium oxide are sensitive to pH, given that protons are involved in the Ir^{4+}/Ir^{3+} equilibrium reactions.

The data suggest inherent implantation variability in blood-brain barrier disruption, which may not be noticeable from the cortical surface. Thus, the results from this study reveal a unique ability to diagnose acute tissue trauma of neural probe implants in real-time. Integrating such technology in a closed-loop drug delivery system may prove beneficial to heal the neural interface more effectively [18].

Acknowledgment

The authors thank Brendan Casey, Ning Gulari, and Jamie Hetke for probe fabrication and packaging; Olivia Kao for surgical assistance, the Neural Engineering Laboratory, Dr. Robert Kennedy, and Kristin Schultz for helpful discussion.

References

[1] A. Prochazka, V. K. Mushahwar, and D. B. McCreery, "Neural prostheses," *J Physiol*, vol. 533, pp. 99-109, 2001.

[2] A. B. Schwartz, "Cortical neural prosthetics," *Annu Rev Neurosci*, vol. 27, pp. 487-507, 2004.

[3] X. Liu, et al., "Stability of the interface between neural tissue and chronically implanted intracortical microelectrodes," *IEEE Trans Rehabil Eng*, vol. 7, pp. 315-26, 1999.

[4] P. J. Rousche and R. A. Normann, "Chronic recording capability of the Utah Intracortical Electrode Array in cat sensory cortex," *J Neurosci Methods*, vol. 82, pp. 1-15, 1998.

[5] R. J. Vetter, et al., "Chronic neural recording using silicon-substrate microelectrode arrays implanted in cerebral cortex," *IEEE Trans Biomed Eng*, vol. 51, pp. 896-904, 2004.

[6] J. C. Williams, R. L. Rennaker, and D. R. Kipke, "Long-term neural recording characteristics of wire microelectrode arrays implanted in cerebral cortex," *Brain Res Protoc*, vol. 4, pp. 303-13, 1999.

[7] M. D. Johnson, K. J. Otto, and D. R. Kipke, "Repeated voltage biasing improves unit recordings by reducing resistive tissue impedances," *IEEE Trans Neural Syst Rehabil Eng*, vol. 13, pp. 160-5, 2005.

[8] Y. Katayama, et al., "Massive increases in extracellular potassium and the indiscriminate release of glutamate following concussive brain injury," *J Neurosurg*, vol. 73, pp. 889-900, 1990.

[9] D. R. Groothuis, et al., "Changes in blood-brain barrier permeability associated with insertion of brain cannulas and microdialysis probes," *Brain Res*, vol. 803, pp. 218-30, 1998.

[10] H. K. Kimelberg, "Current concepts of brain edema. Review of laboratory investigations," *J Neurosurg*, vol. 83, pp. 1051-9, 1995.

[11] R. K. Narayan, et al., "Clinical trials in head injury," *J Neurotrauma*, vol. 19, pp. 503-57, 2002.

[12] L. D. Burke and R. A. Scannell, "Acid-base reactions of oxides and their effect on equilibrium potentials," *J Electrochem Soc*, vol. 131, pp. C298-C298, 1984.

[13] L. D. Burke and R. A. Scannell, "An investigation of hydrous oxide-growth on iridium in base," *J Electroanal Chem*, vol. 175, pp. 119-141, 1984.

[14] A. Fog and R. P. Buck, "Electronic semiconducting oxides as pH sensors," *Sensors and Actuators*, vol. 5, pp. 137-146, 1984.

[15] M. D. Johnson, et al., "Neural probes for concurrent detection of neurochemical and electrophysiological signals in vivo," *Proceedings IEEE Engin Med Bio Soc*, 2005.

[16] L. D. Burke, J. K. Mulcahy, and D. P. Whelan, "Preparation of an Oxidized Iridium Electrode and the Variation of Its Potential with Ph," *Journal of Electroanalytical Chemistry*, vol. 163, pp. 117-128, 1984.

[17] A. K. Gupta, et al., "Extracellular brain pH and outcome following severe traumatic brain injury," *J Neurotrauma*, vol. 21, pp. 678-84, 2004.

[18] S. T. Retterer, et al., "Model neural prostheses with integrated microfluidics: a potential intervention strategy for controlling reactive cell and tissue responses," *IEEE Trans Biomed Eng*, vol. 51, pp. 2063-73, 2004.